WATER RESOURCES RESEARCH, VOL. 36, NO. 7, PAGES 1737–1746, JULY 2000

Transient film flow on rough fracture surfaces

Tetsu K. Tokunaga and Jiamin Wan

Earth Sciences Division, Lawrence Berkeley National Laboratory, Berkeley, California

Stephen R. Sutton

Department of Geophysical Sciences and Consortium for Advanced Radiation Sources, University of Chicago Chicago, Illinois

Abstract. Transient film flow in unsaturated fractures was investigated conceptually and experimentally. By considering films on fracture surfaces as analogs to water in partially saturated porous media, the film hydraulic diffusivity and equation for transient film flow are obtained from their porous medium counterparts, the hydraulic diffusivity and the Richards equation. Experiments on roughened glass show that the average film thickness dependence on matric potential can be approximated as a power function. It is also shown that the film hydraulic diffusivity increases with increased film thickness (and with increased matric potential). Fast film flow (average velocities greater than 3×10^{-7} m s^{-1} under unit gradient conditions) was observed for average film thicknesses greater than 2 μm and matric potentials greater than -1 kPa.

1. Introduction

The nature of water flow in unsaturated fractured rock is complex and incompletely understood. In recent years the phenomenon of fast, preferential flow through the vadose zone has been identified in a wide range of soil and rock types. Various mechanisms have been suggested, including macropore flow [e.g., *Beven and Germann*, 1981; *White*, 1985], fracture flow [e.g., *Nitao and Buscheck*, 1991; *Wang et al.*, 1993], flow fingering in soils and along fractures [*Parlange and Hill*, 1976; *Glass and Nicholl*, 1996], and funneled flow [*Kung*, 1993]. Earlier conceptual models of flow in partially saturated fractures have assumed that local aperture segments must be either fully water saturated or fully desaturated [*Wang and Narasimhan*, 1985; *Pruess and Tsang*, 1990]. In such models, local aperture saturation is assumed to be a strict function of capillary pressure. In these models, flow along the fracture plane could only occur through a network of locally saturated regions. Thus, in aperture-based models, flow is essentially conceptualized as saturated flow within tortuous pathways in fractures.

Recently, the concept of film flow was introduced as a possible process by which preferential flow could occur along truly unsaturated fractured rock. *Kapoor* [1994] investigated the case of free surface flow on a fracture surface. That study implicitly considers water films under a small (positive) pressure potential and includes imbibition into the rock matrix. Our work concerns water films on fracture surfaces under near-zero (negative) matric potentials and examines the possibility of fast unsaturated flow under "tension" [*Tokunaga and Wan*, 1997]. "Films" in this latter context are a complex network of thick pendular regions that form within topographic depressions and thin films on topographic ridges. Thus the thickness and connectivity of pendular film regions is expected to be important in controlling film flow on individual fracture surfaces. We showed that at matric potentials greater than that needed to saturate the rock matrix, transmissive water films can develop on fracture surfaces. The matric potential dependence of the average film thickness and film transmissivity of a Bishop Tuff fracture surface were measured using equilibrium and steady state methods, respectively. The water films investigated in the previous study as well as the present one develop on rough surfaces, range in average thickness from about 1 to 50 μm, and flow in the laminar regime. In the present paper, additional concepts and experimental tests of film flow are presented. These new developments include introduction of the film hydraulic diffusivity and transient film flow equation and new methods for measuring relations between average film thickness, matric potential, and film hydraulic diffusivity.

Since interest in understanding film flow was largely motivated by the need to understand fast flow in unsaturated fractured rock, it will be useful to propose an approximate threshold velocity above which film flow may be considered "fast." As a reference point we will select an average film velocity of 3×10^{-7} m s^{-1} (10 m yr^{-1}) as the criterion for fast flow. Such a velocity would permit transport through a substantial 100-m-thick vadose zone within 1 decade, a relatively short time from the point of view of seepage in arid and semiarid regions. Before describing experimental procedures, aspects of transient film flow will be considered. Having a context for characterizing nonsteady state film flow is valuable not only because a wide range of vadose zone flow is transient in nature, but also because a variety of transient laboratory methods for quantifying film flow can be developed.

2. Transient Film Flow and the Film Hydraulic Diffusivity

Since film flow in many ways appears to be a surface analog to flow in bulk unsaturated porous media, the macroscopic relations useful for describing film flow are expected to be surface analogs of the Darcy-Buckingham law and the Richards equation. Previously [*Tokunaga and Wan*, 1997], film flow was considered from the perspective of steady state flow, with the hydraulic potential gradient as the driving force. In that context the appropriate surface transport coefficient linking

Paper number 2000WR900079.
0043-1397/00/2000WR900079$09.00

volumetric flux per macroscopic fracture length, J [L^3 L^{-1} T^{-1}], to the hydraulic head gradient [L L^{-1}] is the film transmissivity T [L^2 T^{-1}]. In our previous study as well as the present one, we consider the film thickness f [L] as a local areal thickness, averaged over thick capillary films within topographic depressions and thin films on topographic ridges. While film transport processes are expected to be controlled by flow within interconnected channels, we attempt to maintain a macroscopic continuum presentation. This macroscopic perspective is preferred here since our current understanding of microscale film flow over complex fracture surfaces remains qualitative and since we lack experimental methods for quantitative microscale measurements. A number of microscale tests of flow on smooth surfaces [e.g., *Cazabat et al.*, 1990; *Leger and Joanny*, 1992] and on surfaces with simple channel topography have been performed [e.g., *Pozrikidis*, 1988; *Ransohoff and Radke*, 1988; *Zhao and Cerro*, 1992; *Romero and Yost*, 1996; *Rye et al.*, 1996]. In a macroscopic approach to film flow the appropriate averaging distances for continuum hydraulic properties will generally depend on the topography of the surface in question and can be complicated by the scale dependence of surface roughness, as noted in a later section. We assume here that a local measurement encompasses a large population of hydraulically significant topographic oscillations. It may sometimes be useful to consider film flow from the perspective of gradients in average film thickness [L L^{-1}] rather than gradients in hydraulic head as the driving force. The appropriate transport coefficient is then the film hydraulic diffusivity $D(f)$ [L^2 T^{-1}], which is related to the film transmissivity and the film thickness dependence on matric head, h_m [L], through

$$D(f) = \frac{T(f)}{(df/dh_m)}. \tag{1}$$

As shown previously [*Tokunaga and Wan*, 1997], the relation between average film thickness and matric potential for fracture surfaces of wettable porous media is practically nonhysteretic. Thus, for such surfaces, both $T(f)$ and $D(f)$ are also nonhysteretic. The one-dimensional film flux in the vertical direction is

$$J = -D(f)\frac{\partial f}{\partial z} - T(f) \tag{2a}$$

and in the horizontal direction is

$$J = -D(f)\frac{\partial f}{\partial x}. \tag{2b}$$

It should be noted that gradients in average film thickness can only be useful for predicting film flow on macroscopically homogeneous surfaces, just as gradients in volumetric water content can only be applied to predict unsaturated flow within macroscopically homogeneous regions of porous media. Note from (2a) that the steady, unit gradient, gravity-driven film flow per transverse length of macroscopically homogeneous fracture surface is given by $-T(f)$, since macroscopic gradients in film thickness vanish, and that under such conditions the average film velocity is given by $-T/f$.

Since flow in natural systems often takes place under transient conditions, it is useful to have concepts and analytical and experimental methods for characterizing transient film flow. Under conditions of laminar flow, transient film flow can be described in a manner directly analogous to the Richards equation routinely applied to transient unsaturated flow in porous media. For simplicity, we will consider only cases of one-dimensional flow along the z direction, without matrix imbibition and evaporation-condensation. Volumetric fluxes rather than mass fluxes of water will be described since film flows over large variations in absolute pressure, temperature, or solution chemistry are not considered here. The reference volume is depicted in Figure 1. The instantaneous rate of change of water volume within the film is

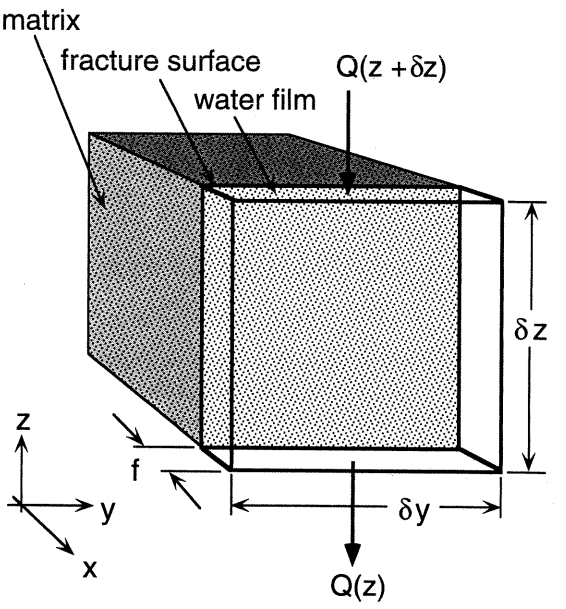

Figure 1. Reference volume for developing transient film flow relations.

$$\frac{\partial V_w}{\partial t} = \delta y \delta z \frac{\partial f}{\partial t}, \tag{3}$$

where f is the average film thickness and V_w is the volume of water. The change in water film volumetric flux along the macroscopic vertical flow path is

$$-\frac{\partial Q}{\partial z}\delta z = \delta y \frac{\partial}{\partial z}\left[T(f)\frac{\partial H}{\partial z}\right]\delta z, \tag{4}$$

where Q is the volumetric water flow rate (positive upward) and H is the hydraulic head ($H = h_m + z$). From continuity, (3) and (4) are equal, leading to

$$\frac{\partial f}{\partial t} = \frac{\partial}{\partial z}\left[T(f)\frac{\partial H}{\partial z}\right] \tag{5a}$$

$$\frac{\partial f}{\partial t} = \frac{\partial}{\partial z}\left[T(f)\left(\frac{\partial h_m}{\partial z} + 1\right)\right]. \tag{5b}$$

When gravity is negligible (horizontal film flow, and short distances, in general), transient film flow with variable T is described by

$$\frac{\partial f}{\partial t} = \frac{\partial}{\partial x}\left[T(f)\frac{dh_m}{df}\frac{\partial f}{\partial x}\right] \tag{6a}$$

and with the chain rule gives

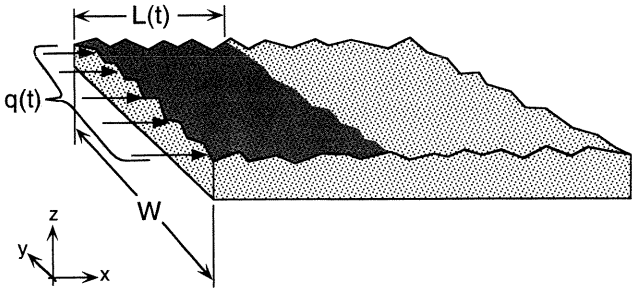

Figure 2. Green-Ampt film model. Transient, one-dimensional film flow is approximated as an advancing step-function film, with instantaneous front position at $L(t)$, and with film uniform thickness.

$$\frac{\partial f}{\partial t} = \frac{\partial}{\partial x}\left[T(f)\left(\frac{\partial h_m}{\partial x}\right)\right]. \tag{6b}$$

By combining the definition of the film hydraulic diffusivity (equation (1)) and (6b), we obtain the transient film flow diffusion equation:

$$\frac{\partial f}{\partial t} = \frac{\partial}{\partial x}\left[D(f)\,\frac{\partial f}{\partial x}\right]. \tag{7}$$

When $D(f)$ is approximately constant, (7) simplifies to the linearized form

$$\frac{\partial f}{\partial t} = D_a\,\frac{\partial^2 f}{\partial x^2}, \tag{8}$$

where D_a is the average film hydraulic diffusivity. While we make use of transient film flow relations where gravity is negligible for purposes of experimental characterization of film hydraulic properties, it is important to recognize the dominant influence of gravity in larger-scale flow.

3. Green-Ampt Analysis of Transient Film Spreading Onto Dry Surfaces

Transient film flow can be studied through measuring the rate of film spreading on initially dry, hydrophilic surfaces. We consider surfaces of impermeable solids such that matrix imbibition of water is unimportant, permitting isolation of film dynamics. Visual observation of wetting on such surfaces has indicated that advancing wetting fronts of films are often quite sharp, so that they may be approximated as step-function wetting profiles. A simple model for transient film flow under the step-function approximation can be developed in a manner analogous to that of the early infiltration model of *Green and Ampt* [1911]. The case of transient, one-dimensional horizontal film flow will be considered here (Figure 2). The rate of film advance (dL/dt) in the step-function approximation is equated with the instantaneous flux at the inflow boundary (Q), such that

$$Q = Wf_a\,\frac{dL}{dt}, \tag{9}$$

where f_a is the constant average film thickness, L is the wetted distance along the direction of flow, and W is the macroscopic wetted length transverse to the flow direction. This flow rate is equated with product of W, T, and the magnitude of the effective matric head gradient,

$$Q = -WT\,\frac{h_{m,f}}{L}, \tag{10}$$

where T is the wetted profile average transmissivity, L is the wetted length along the direction of flow, and $h_{m,f}$ is the effective wetting front matric head. In the above equation the matric head at the inflow boundary is not included because it was set to a nearly zero value in the experiments described later. Combining (9) and (10) gives

$$\frac{dL}{dt} = -\frac{Th_m}{f_a L}, \tag{11}$$

which upon integration results in

$$L(t) = \sqrt{2D_{\mathrm{GA}}t}, \tag{12}$$

where the Green-Ampt (GA) film hydraulic diffusivity is defined as

$$D_{\mathrm{GA}} = \frac{T}{(-f_a/h_f)}. \tag{13}$$

The Green-Ampt film hydraulic diffusivity can be determined during a transient wetting process from the slope of L versus the square root of time (equation (12)). Note that this transient film flow process is the surface analog to one-dimensional infiltration or absorption, such that the film cumulative infiltration I [$L^3\ L^{-1}$] is

$$I = f_a\sqrt{2D_{\mathrm{GA}}t}. \tag{14}$$

Since both cumulative absorption and cumulative short-term infiltration in homogeneous porous media are given by the product of the sorptivity S [$L\ T^{-1/2}$] times the square root of time [*Philip*, 1969], the analogous film flow expression has the identical form

$$I = S_f\sqrt{t} \tag{15}$$

but with different dimensions for the film sorptivity S_f [$L^2\ T^{-1/2}$]. This film sorptivity depends on surface hydraulic properties (T and D), along with initial and boundary film thicknesses (or matric potentials), just as is the case for transient wetting in porous media. Combining (14) and (15), the film thickness, Green-Ampt film hydraulic diffusivity, and S_f are related through

$$D_{\mathrm{GA}} = \frac{S_f^2}{2f_a^2}. \tag{16}$$

4. Film Hydraulic Diffusivities From Suction Plate Outflow

In addition to analysis based on the Green-Ampt approach, we considered three methods previously developed for determining hydraulic diffusivities of partially saturated porous media that recognized dependence on volumetric water content. These methods all use either a pressure plate or suction plate device to impose step changes in potentials along one end of a sample which is in contact with a porous, water-permeable plate [*Klute*, 1986]. The first method, proposed by *Gardner* [1956], assumes that a constant D can be assigned to relatively small but measurable changes in water content (in our case, film thickness). Since this assumption is somewhat restrictive, only some of its most basic aspects will be examined and applied to one set of data for the purpose of comparison with other methods. This method was originally developed using the

matric potential as the time-dependent variable, but as noted by *Marshall and Holmes* [1979], it can be applied to the water content as well (saturation and potential are assumed to be linearly related over short increments measured in individual tests). It applies in the case of film flow to transient, one-dimensional flow on finite length (L) surfaces, initiated by a step change in film thickness at the boundary in contact with a pressure plate or suction plate. In the case of transient film flow in a suction plate device, the appropriate initial and boundary conditions are

$$\begin{aligned} f &= f_i, \quad 0 \le x \le L, \quad t = 0 \\ f &= f_f, \quad x = 0, \quad t > 0 \\ df/dx &= 0, \quad x = L, \quad t > 0. \end{aligned} \tag{17}$$

For constant D, the solution to (8) and (17) is given by a Fourier series in which only the first term is significant after $t > 0.1L^2/D$. After such time, the average film thickness is given by

$$f(t) = f_f + \frac{8}{\pi^2}(f_i - f_f)\exp\left(\frac{-\pi^2 Dt}{4L^2}\right). \tag{18}$$

The D obtained by fitting the above equation will later be referred to as a result of Gardner's method 1.

A second, more general method for determining hydraulic diffusivities in soils was also proposed by *Gardner* [1962], again applicable to outflow from a pressure plate, pressure membrane, or suction plate device. A varying hydraulic diffusivity, dependent on water content (film thickness), is obtained with this method and will be referred to as Gardner's method 2. It applies in the case of film flow to transient, one-dimensional flow on finite length (L) surfaces, initiated by a step change in film thickness at one boundary in contact with a pressure plate or suction plate. The solution to (7), subject to the same initial and boundary conditions (equation (17)), is

$$D(f) = \frac{4L^2}{(f - f_f)\pi^2}\frac{df}{dt}. \tag{19}$$

The final method applied in this study is that of *Passioura* [1976], which evaluates the hydraulic diffusivity at the end of the soil column ($x = L$), based on the change in the rate of water loss with change in average water content. Passioura showed that his analysis agreed well with numerical simulations of outflow experiments (typically calculating D to within 5% of true values but overestimating by about 25% as equilibrium is approached). In terms of a transient, suction plate experiment, the *Passioura* [1976] method determines the film hydraulic diffusivity through

$$D(f_L) = \frac{L^2}{2}\frac{dQ}{df_a}, \tag{20}$$

where

$$Q = -\frac{\partial f}{\partial t} \approx -\frac{\partial f_a}{\partial t} \tag{21}$$

$$f_L \approx f_a - 0.61\frac{df_a}{d\ln D(f_L)}, \tag{22}$$

where f_a is the average film thickness, measured within the central region of a test surface. In the experimental section, film hydraulic diffusivities will be determined using each of these methods, i.e., by applying (16), (18), (19), and (20)–(22).

5. Experimental Samples

To isolate film flow effects from flow within the underlying matrix, it is desirable to conduct experiments on surfaces of impermeable solids. Although it is possible to conduct film flow experiments on permeable rock, additional tests are required to characterize the matrix contribution to flow [*Tokunaga and Wan*, 1997]. Subtraction of the matrix flow component for purposes of isolating film flow on permeable surfaces limits the accuracy of this approach, because of uncertainty in the matrix flux. Thus, for purposes of testing concepts, two types of impermeable glasses were used: a glass cast of a granite fracture surface and a roughened glass plate. The glass cast provided a water-wettable, transparent, nonporous surface that closely replicates the surface topography of the original granite fracture. The casting method, photographs of glass casts, and results of various hydraulic experiments on casts are given by *Wan et al.* [2000]. The roughened glass surface consisted of a 3.2-mm-thick glass plate, abraded on one side with 80-grit silicon carbide. Both the glass cast and roughened glass samples used in the Green-Ampt wetting experiments were 120 × 160 mm in bulk surface area. Suction plate experiments were only done on a roughened glass sample since the analytical procedure assumes a macroscopically homogeneous surface. For these latter experiments, a much smaller, 6-mm-tall × 15-mm-wide × 3-mm-thick, sample was prepared in the same way as the larger, 80-grit abraded glass plate.

Roughness measurements were obtained with an atomic force microscope (Autoprobe M5, Park Scientific Instruments, Sunnyvale, California) and a laser profilometer (UBM, Sunnyvale, California) for fine-scale features and with a laser profilometry (LK-081 CCD laser displacement sensor, Keyence Corp., Woodcliff Lake, New Jersey) on coarser, long-range features. The Autoprobe M5 has a resolution of 0.025 nm and a lateral range of 100 × 100 μm. However, since the maximum measurable z variation of this atomic force microscope is only 8 μm, scans on rough surfaces must be confined to even smaller areas than the instrument's 100-μm × 100-μm range. The UBM laser has a spot size of 1 μm, a z measurement range of 100 μm, and a z resolution of 0.06 μm. The LK-081 laser has a vertical (z) measurement range of 30 mm, a spot diameter of about 70 μm, and an uncertainty of ±35 μm in z. The View Precis 3000 coordinate measuring machine used on both of the laser systems has resolution and repeatability in the x-y plane of ±3 μm. Like natural fractures [*Brown and Scholz*, 1985; *Power and Tullis*, 1991], the cast exhibits scale-dependent roughness, with measured values of the root-mean-square roughness (rmsr) ranging from 4 to 7 μm (over 20-μm scans), from 600 to 800 μm (over 10-mm scans), and from 2 to 3 mm (over 100-mm scans). The silicon carbide-roughened glass surface had a stationary (scale-independent) rmsr of 9 μm for scan lengths greater than 500 μm. Examples of roughness profiles of glass casts and roughened glass are given by *Wan et al.* [2000].

6. Measurement of the Green-Ampt Film Hydraulic Diffusivity

Measurements of horizontal film advance over two initially dry surfaces, one of a glass cast of a granite fracture surface and the other of a roughened glass plate, were performed within a sealable acrylic plastic chamber (Figure 3a). The inflow water source consisted of a saturated, 0.5-bar, high-flow ceramic block (Soilmoisture Equipment Corp., Santa Barbara,

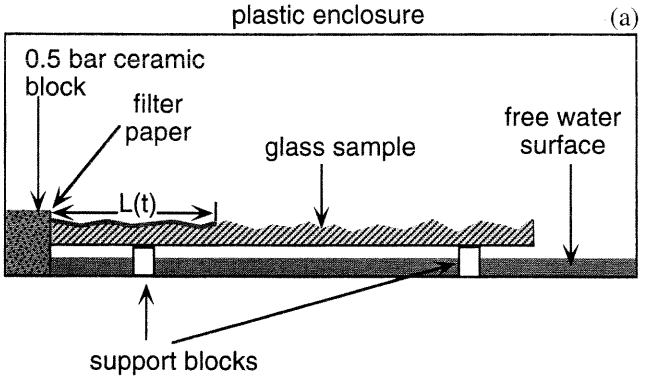

(b)

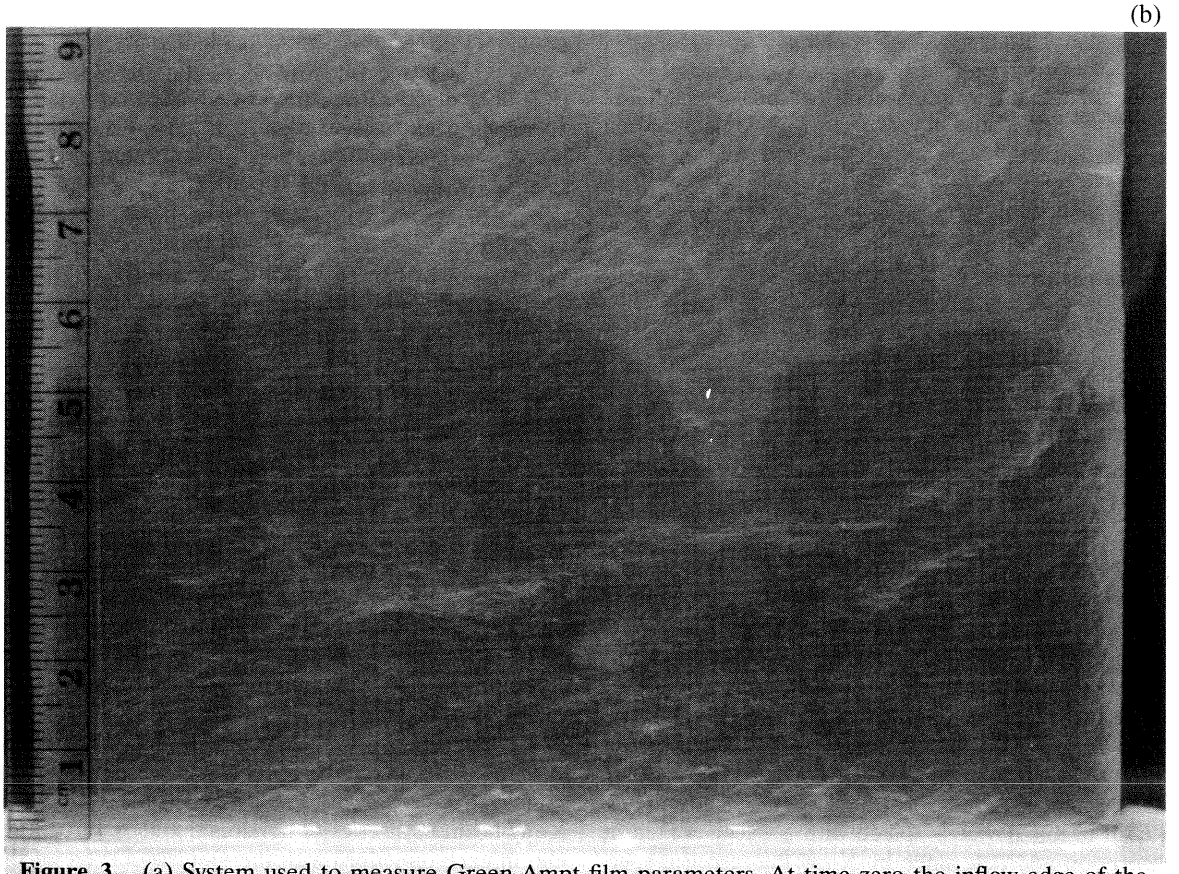

Figure 3. (a) System used to measure Green-Ampt film parameters. At time zero the inflow edge of the sample is contacted to the water reservoir, and $L(t)$ is visually recorded. (b) Photograph of a wetting front advancing on a glass cast fracture surface.

California) in contact with a free water reservoir. A layer of coarse filter paper is placed over the ceramic to provide good hydraulic contact between the ceramic and the test sample. The filter paper interface probably also significantly lowered the boundary source hydraulic resistance since it also wicks water up directly from the free water reservoir. The sample is supported horizontally, above the free water surface, with plastic blocks. At time zero, the $x = 0$ edge of the sample is placed in contact with the filter-covered ceramic plate, and the visually observed wetting front position (minimum, average, and maximum) is recorded as a function of time (Figure 3b). The matric head at the inflow boundary was -6 mm for the roughened glass plate and -12 ± 5 mm for the glass cast. The variability in the latter was due to topographic variations along the $x = 0$ edge of the cast. At the end of the experiment the sample was quickly placed on an electronic balance within an acrylic plastic, humidified box, to determine the cumulative mass of water imbibed onto the test surface.

7. Measurement of Film Thickness and Its Relation to Matric Potential and Hydraulic Diffusivities With a Suction Plate Device

Since a wide variety of suction plate and pressure plate methods have been successfully used for determination of hydraulic properties of partially saturated porous media, a modified version of the suction plate was developed for purposes of measuring film hydraulic properties on rough surfaces. This

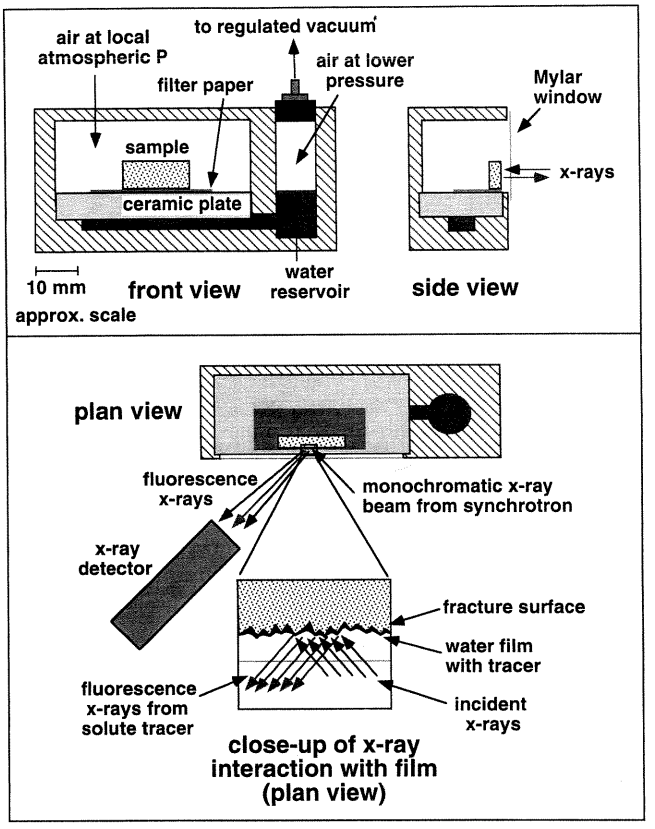

Figure 4. Sample cell for synchrotron X-ray fluorescence measurements of film thickness versus matric potential.

device (Figure 4) is designed to measure equilibrium relations between matric potential and average film thickness and to measure film hydraulic diffusivities on surfaces of impermeable solids through X-ray fluorescence of a solute tracer. A small block of the roughened glass is placed on top of a high-conductance ceramic plate (0.5 bar, Soilmoisture Equipment Corp., Santa Barbara, California), with the roughened glass surface oriented vertically. Filter paper is placed between the sample and ceramic to improve hydraulic contact. The aqueous solution used in this device is spiked with a tracer excited by X-ray absorption and detectable by X-ray fluorescence spectrometry. The tracer used in this experiment was selenate (SeO_4^{2-}), added as a sodium salt at a concentration of 242 mM. The selection of Se as a tracer was based on its large K-edge X-ray fluorescence yield of 60% [*Kostroun et al.*, 1971] and its very low fluorescent X-ray absorbance by the Mylar film used for the sample chamber window. The choice of SeO_4^{2-} in particular was based on its very low affinity to most mineral surfaces [*Neal and Sposito*, 1989]. The sample, ceramic plate, and solution reservoir are contained within an acrylic plastic block, sealed to minimize evaporation, but with the sample housing pinhole-vented to maintain the air in equilibrium with local atmospheric pressure. The Mylar film window sealing the front face of the sample housing permits incident and fluorescent X-ray fluxes with insignificant attenuation at the photon energies used. The regulated pressure of the air headspace overlying the tracer reservoir solution is monitored continuously with a pressure transducer (Tensimeter, Soil Measurement Systems, Tucson, Arizona). The matric potential at the ceramic surface is controlled by regulating the subatmospheric pressure of the air headspace in the solution reservoir. This is done through removal or injection of air via a syringe while its hypodermic needle is inserted into a septum stopper and while monitoring the pressure transducer display.

Experiments were conducted at beamline X26A of the National Synchrotron Light Source (NSLS), Brookhaven National Laboratory [*Sutton et al.*, 1994; *Sutton and Rivers*, 1999]. Overviews of synchrotron X-ray applications in Earth sciences are given by *Brown and Parks* [1989], *Schulze and Bertsch* [1995], and *Smith and Rivers* [1995]. A brief description of pertinent operating conditions for this experiment is provided here. The monochromator was set to 12.70 keV, about 34 eV above the Se(VI) K absorption edge. Although this beamline is routinely used as an X-ray microprobe and for microspectroscopy with spot sizes down to 5 μm, the focusing optics were removed during these experiments in order to utilize a much broader incident X-ray beam of about 200 μm. The larger spot size was preferred in the present application since it permitted averaging over greater areas of the rough surface and maximized the incident X-ray flux. X-ray fluorescence from the selenate in the water film was measured with an energy dispersive detector (lithium-drifted silicon). Blank measurements on a quartz glass block prior to exposure to selenium confirmed that matrix Se concentrations were below detection. The average water film thickness from a given measurement was calculated from a linear calibration curve constructed from standards with known Se surface concentrations (Se mass per unit area). These standard samples were prepared by micropipetting selected amounts of selenate solutions onto small filter paper pads (ranging in area from 4 to 25 mm^2). The resulting areal Se concentrations ranged from 7.8 to 94 ng mm^{-2}, and equivalent film thicknesses ranged from 0.82 to 9.8 μm for the 242-mM solution. Standard samples were scanned with the X-ray microprobe to obtain the areal distribution of Se within each pad. Edges of filter pads showed 20–30% enrichment of the Se tracer due to enhanced evaporation and about 10% relative depletion from central regions. The spatial map of Se concentrations on each pad was averaged for use in later film thickness calculations.

A range of matric potentials from -0.3 to -50 kPa was examined. For an equilibration at a given matric potential, the sample chamber was rastered in front of the stationary incident X-ray beam in a series of horizontal and/or vertical steps (0.5 mm in each direction) with the motorized stage of the X26A end station. This procedure permitted areal averaging of X-ray fluorescence within the central 3-mm $\times$ 3-mm region of the roughened surface. Measurements at a given spot on the rough glass surface were obtained within 5–15 s. Energy balance calculations indicate that the local temperature increase under these operating conditions was less than 1°C. Rastering of the sample relative to the X-ray beam permitted areal averaging of film thickness measurements as well as minimization of local thermal loading from the incident beam. For a given step change in boundary matric potential, the sample was periodically scanned until the average Se X-ray fluorescence signal became constant, indicating equilibrium. The observed stable equilibrium fluorescence indicated that thermal loading from the X-ray beam had only a minor effect on these measurements. The equilibrium average film thickness at the prescribed matric potential was calculated from the equilibrium Se X-ray fluorescence intensity (normalized to the incident photon flux and count time) by referencing the calibration samples. Transient film thinning results were used to deter-

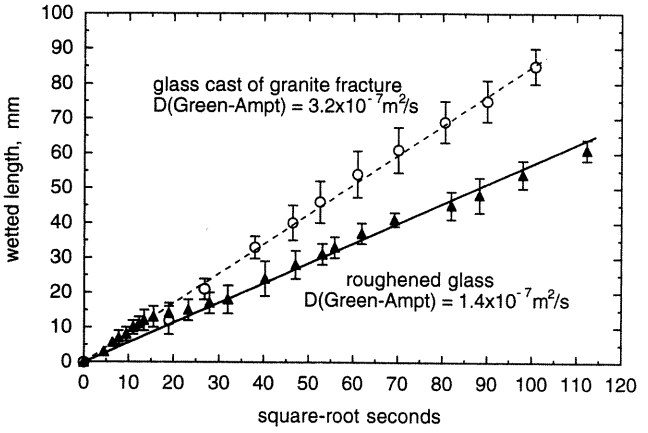

Figure 5. Wetting front distance versus square root of time for film flow over a roughened glass surface, and a glass cast of a granite fracture surface. Data points indicate average front positions. Range bars indicate approximate ranges in wetting front positions.

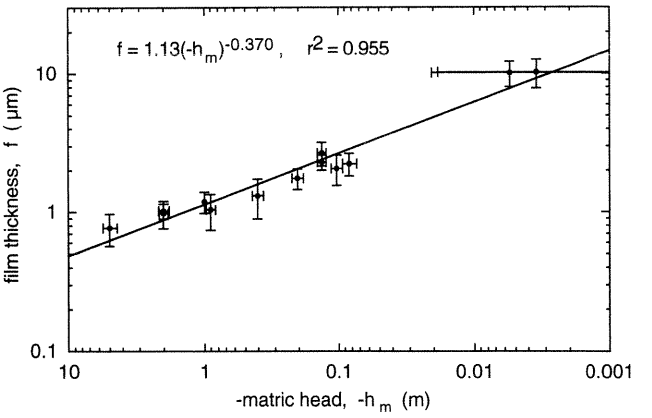

Figure 6. Film thickness versus matric head, for the roughened glass surface, measured with synchrotron X-ray fluorescence of a selenate tracer.

mine film hydraulic diffusivities according to procedures previously described (equations (18)–(22)).

8. Results and Discussion

Wetting of the horizontally oriented glass fracture cast and roughened glass plate proceeded without occlusion of residual dry regions. Cumulative water film uptake on the two glass surfaces proceeded in accordance with the expected (equation (12)) square root of time proportionality (Figure 5). The cause of the initially steeper slope for wetting of the roughened glass (for times <15 s$^{1/2}$) is not known. However, it does not suggest that inflow was restricted at the source since this condition would yield a lower initial slope relative to later times in the wetting process. In each case the wetting front of the film was visible as a sharp transition between a translucent wetted region and a more opaque dry surface. Although this boundary was visually sharp, the wetted length varied by up to $\pm 13\%$ of the average front position. The wetted area-averaged film thicknesses on the glass cast and roughened glass were 2.3 ± 0.3 and 2.6 ± 0.2 μm, respectively. From the slope of the film sorptivity plot, the average film thickness, and (18), flow on the glass fracture cast yielded a Green-Ampt film hydraulic diffusivity of 4.6×10^{-7} ($\pm 0.9 \times 10^{-7}$) m^2 s^{-1}. The Green-Ampt film hydraulic diffusivity for the roughened glass surface was 1.3×10^{-7} ($\pm 0.2 \times 10^{-7}$) m^2 s^{-1}.

Time for equilibration of water films on the smaller rough glass sample took from as little as about 10 min in the near-zero matric potential range to over 10 hours for potentials lower than -20 kPa. Equilibrium relations between matric head and synchrotron X-ray-measured average water film thickness on the roughened glass sample are shown in Figure 6. Over the experimental range of -50 to -0.3 kPa in matric potential, average water film thicknesses ranged from 0.75 to 10 μm, respectively. The log-log plot of these data permits comparisons with a power function fit. The power function fit to these fracture surface film data is fairly close, with an exponent of -0.37. Exponents in power law soil water retention relations have been used in fractal analyses of porous media to examine relations between pore structure and equilibrium and transport properties [*de Gennes*, 1985; *Tyler and Wheatcraft*, 1990; *Rieu and Sposito*, 1991a, b; *Bird et al.*, 1996; *Perrier et al.*, 1996]. The manner in which the exponent of a power law fit to film thickness–potential relations may be related to fracture surface structure and to these previous studies of unsaturated porous media is not yet known.

An important difference between the single fracture surfaces investigated here, and porous media, is that the latter have well-defined upper limits for volumetric water content (i.e., the porosity), whereas single fracture surfaces generally do not. The lack of a well-defined upper limit on film thickness, hence also a similar lack of a "saturated" film transmissivity on unbounded (effectively infinite aperture) fracture surfaces, may give rise to difficulties in the application of other porous medium hydraulic relations. For example, Smith-Parlange scaling based on soil infiltration rates requires information on the effective saturated hydraulic conductivity as well as the source flux density associated with surface ponding [*Smith and Parlange*, 1977; *Haverkamp et al.*, 1998]. As another example, several methods (summarized by *Kutilek and Valentova* [1986]) have been developed for calculating sorptivities from the moisture content dependent hydraulic diffusivity, requiring knowledge of saturated properties. A possible resolution of such differences would entail selecting some arbitrary near-zero matric potential for films, in place of saturation.

Transient film drainage measurements on the roughened glass were obtained by periodically monitoring film thicknesses using synchrotron X-ray fluorescence, following a step change of the boundary potential (increased plate suction). Time-dependent changes in film thickness served as the basis for calculating film hydraulic diffusivities using the suction plate apparatus. In the example shown in Figure 7, the initial equilibrium matric potential was -1.2 kPa, and at time zero a potential of -20 kPa was imposed and maintained at the ceramic boundary. The average film thickness decreased from an initial value of 2.3 μm to 1.0 μm. The predicted $f(t)$ obtained using Gardner's method 1, with a best fit $D = 5 \times 10^{-9}$ m^2 s^{-1}, is shown with the X-ray measured data. As seen in the figure, the single value of D obtained with Gardner's first method is best associated with the later stage data, for film thicknesses ranging from 1.3 down to 1.0 μm. Inclusion of higher-order terms of the Fourier series (not shown) provided only a slight improvement of the fit because the model assumes

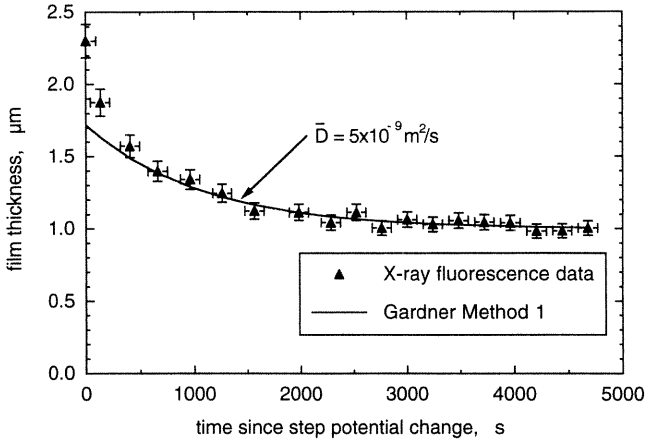

Figure 7. An example of transient water film thinning on roughened glass, in response to a step change in the matric potential at the boundary from −1.2 to −20 kPa.

a constant diffusivity, whereas D decreases with decreasing film thickness.

In order to investigate a wider range of film thickness dependent diffusivities, segments of the continuous $D(f)$ relation were obtained with Gardner's method 2 and with Passioura's method. Results of such calculations are shown in Figure 8, where time-dependent film thinning data are combined with (19) and (20)–(22) to obtain the film hydraulic diffusivity as a function of average film thickness. Both Gardner's second method and the Passioura analyses are plotted for one of the outflow steps in order to permit comparisons. The two methods yielded similar $D(f)$ relations. The Passioura-based analyses were applied to the two other outflow steps also shown in Figure 8, indicating fair reproducibility as well as continuity of results obtained from adjacent segments of $D(f)$. The Green-Ampt integral diffusivity film from the experiment on initially dry rough glass is also plotted in Figure 8, for its associated gravimetrically measured average film thickness. Good agreement is obtained from these two very different approaches. The effective D for the 1.0- to 1.2-μm film thickness range, calculated from Gardner's method 1 (described previously), is also included in Figure 8. Note that it also agrees well with results obtained for variable D.

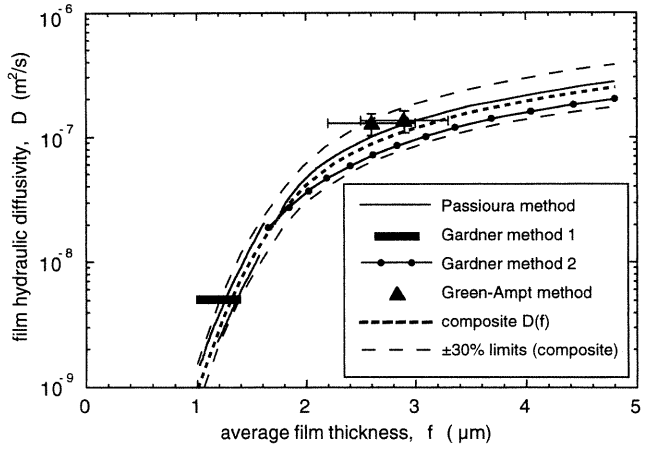

Figure 8. Film hydraulic diffusivity functions for the roughened glass surface, calculated from suction plate outflow measurements. Uncertainties in the *Passioura* [1972] and *Gardner* [1956] method 2 are shown as the bounding dashed lines. Uncertainties in the Gardner method 1 are indicated by the symbol size. Also shown is the film hydraulic diffusivity obtained with the Green-Ampt approach.

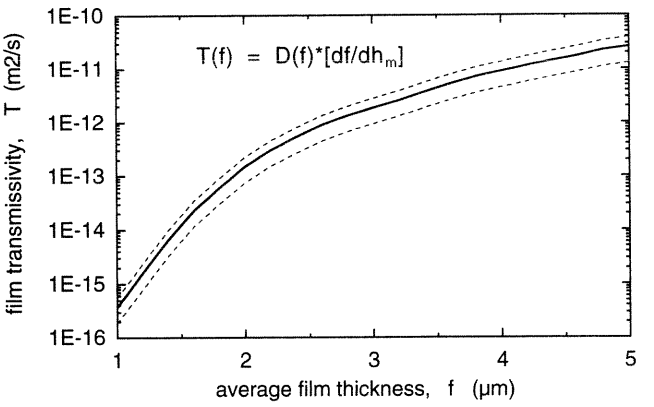

Figure 9. Film transmissivity function $T(f)$ for the roughened glass surface, obtained by multiplying $D(f)$ by df/dh_m.

The measured $D(f)$ shown in Figure 8 collectively exhibit monotonic decreases with decreased film thickness. In the limit of thinner films it might be possible that increased values of D develop, as was first proposed for unsaturated porous media by *de Gennes* [1985], who described such a trend as "hyperdispersion." Hyperdispersive D was predicted by de Gennes for partially saturated porous media in which water was retained primarily in isolated pendular rings and pits and interconnected through thin films. Hyperdispersion has been observed for some porous media by *Bacri et al.* [1985, 1990] and *Toledo et al.* [1993]. In the present case the lack of observation of hyperdispersive $D(f)$ suggests that film flow is controlled by flow along interconnected surface channels rather than by flow in true thin films. Microscopic observations and profilometry of the test surfaces lend support to the expectation that flow occurs primarily through such interconnected surface channels, but future experiments with higher spatial resolution are needed to gain an improved understanding of this aspect.

In order to obtain the film transmissivity and velocity relations for the rough glass surface, the composite $D(f)$ curve (Figure 8) was first multiplied by the first derivative of the power law fit to the $f(h_m)$ relation (Figure 6). This results in the film transmissivity relation shown in Figure 9, along with its estimated range of uncertainty of 50%, obtained by estimating the relative uncertainties in D and df/dh_m to be 30% and 40%, respectively. Dividing this film transmissivity function by its corresponding average film thickness gives the average film velocity, shown as a function of f and h_m in Figures 10a and 10b, respectively. The relative uncertainty in $v(f)$ was estimated to be 54%, based on relative uncertainties for T and f of 50% and 20%, respectively. These results show that average unit gradient film velocities on this impermeable glass surface begin to exceed our selected threshold for fast flow of 10 m yr^{-1} when average film thicknesses are greater than about 2.5 μm and when matric potentials are greater than about −1 kPa. This result, along with our previous work [*Tokunaga and Wan*, 1997], indicates that near-zero matric potentials are required for fast film flow. It should be noted that our currently available database is still very limited, so that comprehensive delineation of conditions needed for fast flow is still premature.

In considering the present results, it should be remembered

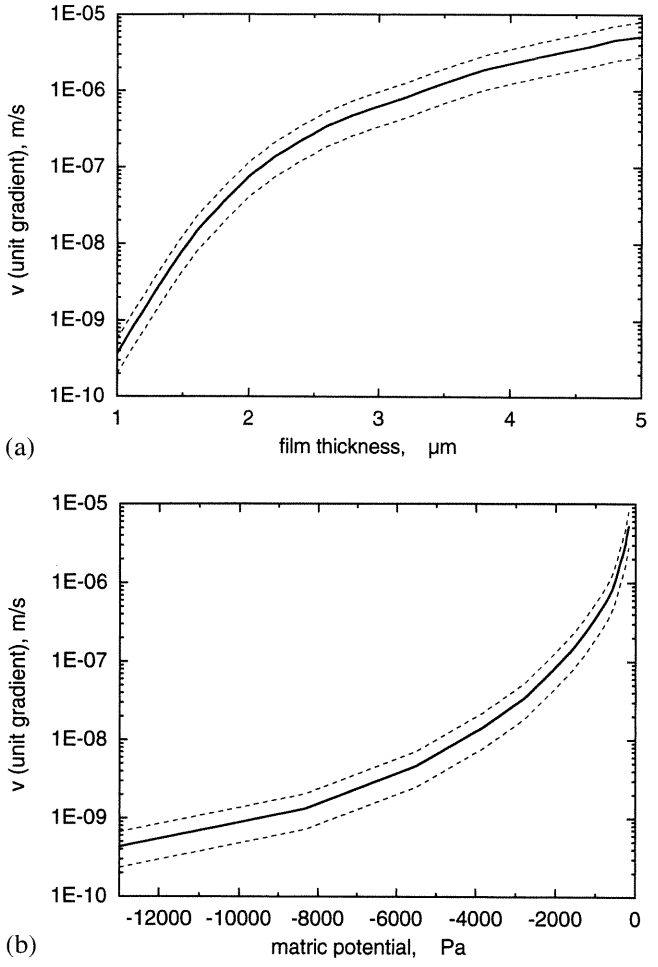

Figure 10. Unit gradient average film velocity for the roughened glass surface, obtained by dividing $T(f)$ by f. Average film velocities are related to (a) average film thickness and (b) film matric head.

that most of the measurements were obtained for a roughened glass surface that is much smoother (9-μm root-mean-square roughness) than many natural fractured rock surfaces (at comparable measurement lengths in the millimeter to centimeter range). Furthermore, since our test surface was artificially roughened by abrasion, its topography is not strongly position dependent and is best characterized as stationary or Euclidian. Natural rock fracture surfaces, on the other hand, have profiles that are typically strongly position dependent and are best described as nonstationary or fractal [e.g., *Power and Tullis*, 1991]. Surfaces with higher roughness are expected to permit thicker films only at very near zero matric potentials, since filling of larger-amplitude fracture surface depressions will be associated with larger radii of air-water interfacial curvature. Note that the inverse relation between matric potential and interfacial curvature, and the scale-dependent fracture surface roughness imply that the area over which continuum film hydraulic properties needs to be averaged increases as zero matric potential is approached.

Further experiments are being designed to improve our understanding of surface roughness influences on film flow, applying the methods presented here to glasses and other mineral surfaces with varying surface roughness. Experiments on single glass fracture cast surfaces and mated glass cast surfaces (at selected values of mean aperture) will also be conducted in order to begin integrating surface and aperture contributions in unsaturated fracture flow.

9. Summary

Aspects of film flow in unsaturated fractures examined in this study included constitutive relations for transient film flow and measurements of film hydraulic parameters under transient conditions. By considering films on fracture surfaces as analogs to water in partially saturated porous media, the film hydraulic diffusivity and equation for transient film flow were obtained from their porous medium counterparts, the hydraulic diffusivity and the Richards equation. Several different measurement techniques, based upon previously developed soil physics methods, were developed for application to studies of film flow. The experiments described in the present study on a roughened glass surface (9-μm root-mean-square roughness) showed the average film thickness dependence on matric potential is approximated as a power function. It was also shown that the film hydraulic diffusivity increases with increased film thickness (and with increased matric potential). Fast film flow, defined here as flow with average velocities greater than 10 m yr^{-1} under unit gradient conditions, was observed for average film thicknesses greater than 2.5 μm and matric potentials greater than -1 kPa on the roughened glass surface.

Acknowledgments. We thank Tom Orr, Andrew Mei, Jim O'Neill, Robert Conners, and Keith Olson, of LBNL, for assistance in parts of this work; Grace Shea-McCarthy, of the University of Chicago, for assistance at NSLS X26A; and Vivek Kapoor for providing a copy of his report. The helpful internal review comments by Garrison Sposito (University of California, Berkeley, and LBNL), Srinivas Veerapaneni (LBNL), and Robert W. Zimmerman (Imperial College, London, and LBNL) are gratefully acknowledged. We also thank Mike Nicholl and two anonymous reviewers for their very helpful suggestions. This work was carried out under U.S. Department of Energy (DOE) contract DE-AC03-76SF00098, with funding provided by the DOE, Basic Energy Sciences, Geosciences Research Program. This work was also supported in part by DOE-Geosciences grant DE-FG02-92ER14244 (S.R.S.). Research was carried out (in part) at the National Synchrotron Light Source, Brookhaven National Laboratory, which is supported by the U.S. Department of Energy, Division of Materials Sciences and Division of Chemical Sciences under contract DE-AC02-98CH10886. We thank the staff of NSLS for providing the synchrotron radiation.

References

Bacri, J.-C., C. Leygnac, and D. Salin, Evidence of capillary hyperdiffusion in two-phase fluid flows, *J. Phys. Lett.*, *46*, L467–L473, 1985.

Bacri, J.-C., M. Rosen, and D. Salin, Capillary hyperdiffusion as a test of wettability, *Europhys. Lett.*, *11*, 127–132, 1990.

Beven, K., and P. F. Germann, Water flow in soil macropores, II, A combined flow model, *J. Soil Sci.*, *32*, 15–29, 1981.

Bird, N. R. A., F. Bartoli, and A. R. Dexter, Water retention models for fractal soil structures, *Eur. J. Soil Sci.*, *47*, 1–6, 1996.

Brown, G. E., Jr., and G. A. Parks, Synchrotron-based X ray absorption studies of cation environments in Earth materials, *Rev. Geophys.*, *27*, 519–533, 1989.

Brown, S. R., and C. H. Scholz, Broad bandwidth study of the topography of natural rock surfaces, *J. Geophys. Res.*, *90*(B14), 12,575–12,582, 1985.

Cazabat, A. M., N. Fraysse, F. Heslot, and P. Carles, Spreading at the microscopic scale, *J. Phys. Chem.*, *94*, 7581–7585, 1990.

de Gennes, P. G., Partial filling of a fractal structure by a wetting fluid, in *Physics of Disordered Materials*, edited by D. Adler, H. Fritzsche, and S. R. Ovshinsky, pp. 227–241, Plenum, New York, 1985.

Gardner, W. R., Calculation of capillary conductivity from pressure plate outflow data, *Soil Sci. Soc. Am. Proc.*, *20*, 317–320, 1956.

Gardner, W. R., Note on the separation and solution of diffusion type equations, *Soil Sci. Soc. Am. Proc.*, *26*, 404, 1962.

Glass, R. J., and M. J. Nicholl, Physics of gravity fingering of immiscible fluids within porous media: An overview of current understanding and selected complicating factors, *Geoderma*, *70*, 133–163, 1996.

Green, W. H., and G. A. Ampt, Studies on soil physics, 1, The flow of air and water through soils, *J. Agric. Sci.*, *4*, 1–14, 1911.

Haverkamp, R., J.-Y. Parlange, R. Cuenca, P. J. Ross, and T. S. Steenhuis, Scaling of the Richards equation and its application to watershed modeling, in *Scale Dependence and Scale Invariance in Hydrology*, edited by G. Sposito, pp. 190–223, Cambridge Univ. Press, New York, 1998.

Kapoor, V., Water film flow in a fracture in unsaturated porous medium, *Rep. CNWRA 94-009*, Cent. for Nucl. Waste Regul. Anal., San Antonio, Tex., May 1994.

Klute, A., Water retention: Laboratory methods, in *Methods of Soil Analysis, Part 1, Physical and Mineralogical Methods*, 2nd ed., edited by A. Klute, pp. 635–662, Agron. Soc. of Am. and Soil Sci. Soc. of Am., Madison, Wisc., 1986.

Kostroun, V. O., M. H. Chen, and B. Crasemann, Atomic radiation transition probabilities to the 1s state and theoretical K-shell fluorescence yields, *Phys. Rev. A*, *3*, 533–545, 1971.

Kung, K.-J. S., Laboratory observation of funnel flow mechanism and its influence on solute transport, *J. Environ. Qual.*, *22*, 91–102, 1993.

Kutilek, M., and J. Valentova, Sorptivity approximations, *Transp. Porous Media*, *1*, 57–62, 1986.

Leger, L., and J. F. Joanny, Liquid spreading, *Rep. Prog. Phys.*, *55*, 431–486, 1992.

Marshall, T. J., and J. W. Holmes, *Soil Physics*, 345 pp., Cambridge Univ. Press, New York, 1979.

Neal, R. H., and G. Sposito, Selenate adsorption on alluvial soils, *Soil Sci. Soc. Am. J.*, *53*, 70–74, 1989.

Nitao, J., and T. Buscheck, Infiltration of a liquid front in an unsaturated fractured porous medium, *Water Resour. Res.*, *27*, 2099–2112, 1991.

Parlange, J.-Y., and D. E. Hill, Theoretical analysis of wetting front instability in soils, *Soil Sci.*, *122*, 236–239, 1976.

Passioura, J. B., Determining soil water diffusivities from one-step outflow experiments, *Aust. J. Soil Res.*, *15*, 1–8, 1976.

Perrier, E., M. Rieu, G. Sposito, and G. de Marsily, Models of the water retention curve for soils with a fractal pore size distribution, *Water Resour. Res.*, *32*, 3025–3031, 1996.

Philip, J. R., Theory of infiltration, *Adv. Hydrosci.*, *5*, 215–296, 1969.

Power, W. L., and T. E. Tullis, Euclidean and fractal models for the description of rock surface roughness, *J. Geophys. Res.*, *96*(B1), 415–424, 1991.

Pozrikidis, C., The flow of a liquid on a periodic wall, *J. Fluid Mech.*, *188*, 275–300, 1988.

Pruess, K., and Y. W. Tsang, On two-phase relative permeability and capillary pressure of rough-walled rock fractures, *Water Resour. Res.*, *26*, 1915–1926, 1990.

Ransohoff, T. C., and C. J. Radke, Laminar flow of a wetting liquid along corners of a predominantly gas-occupied noncircular pore, *J. Colloid Interface Sci.*, *121*, 392–401, 1988.

Rieu, M., and G. Sposito, Fractal fragmentation, soil porosity, and soil water properties, 1, Theory, *Soil Sci. Soc. Am. J.*, *55*, 1231–1238, 1991a.

Rieu, M., and G. Sposito, Fractal fragmentation, soil porosity, and soil water properties, 2, Applications, *Soil Sci. Soc. Am. J.*, *55*, 1239–1244, 1991b.

Romero, L. A., and F. G. Yost, Flow in an open channel capillary, *J. Fluid Mech.*, *322*, 109–129, 1996.

Rye, R. R., J. A. Mann Jr., and F. G. Yost, The flow of liquids in surface grooves, *Langmuir*, *12*, 555–565, 1996.

Schulze, D. G., and P. M. Bertsch, Synchrotron X-ray techniques in soil, plant, and environmental research, *Adv. Agron.*, *55*, 1–66, 1995.

Smith, J. V., and M. L. Rivers, Synchrotron X-ray microanalysis, in *Microprobe Techniques in the Earth Sciences*, *Mineral. Soc. Ser.*, vol. 6, edited by P. J. Potts et al., pp. 163–233, Chapman and Hall, New York, 1995.

Smith, R. E., and J.-Y. Parlange, Optimal prediction of ponding, *Trans. ASAE*, *20*, 493–496, 1977.

Sutton, S. R., and M. L. Rivers, Hard X-ray synchrotron microprobe techniques and applications, in *Synchrotron X-Ray Methods in Clay Science*, *Clay Miner. Soc. Workshop Lect.*, vol. 9, edited by D. G. Schulze, J. W. Stucki, and P. M. Bertsch, pp. 146–163, Clay Miner. Soc., Boulder, Colo., 1999.

Sutton, S. R., M. L. Rivers, S. Bajt, K. Jones, and J. V. Smith, Synchrotron X-ray fluorescence microprobe: A microanalytical instrument for trace element studies in geochemistry, cosmochemistry, and the soil and environmental sciences, *Nucl. Instrum. Methods Phys. Res. A*, *347*, 412–416, 1994.

Tokunaga, T. K., and J. Wan, Water film flow along fracture surfaces of porous rock, *Water Resour. Res.*, *33*, 1287–1295, 1997.

Toledo, P. G., H. T. Davis, and L. E. Scriven, Capillary hyperdispersion of wetting liquids in fractal porous media, *Transp. Porous Media*, *10*, 81–94, 1993.

Tyler, S. W., and S. W. Wheatcraft, Fractal processes in soil water retention, *Water Resour. Res.*, *26*, 1047–1054, 1990.

Wan, J., T. K. Tokunaga, T. Orr, J. O'Neill, and R. W. Conners, Glass casts of rock fracture surfaces: A new tool for studying flow and transport, *Water Resour. Res.*, *36*, 355–360, 2000.

Wang, J. S. Y., and T. N. Narasimhan, Hydrologic mechanisms governing fluid flow in a partially saturated, fractured, porous medium, *Water Resour. Res.*, *21*, 1861–1874, 1985.

Wang, J. S. Y., N. G. W. Cook, H. A. Wollenberg, C. L. Carnahan, I. Javandel, and C. F. Tsang, Geohydrological data and models of Ranier Mesa and their implications to Yucca Mountain, in *High Level Radioactive Waste Management, Proceedings of the 4th Annual International Conference*, vol. 1, pp. 675–681, Am. Nucl. Soc., LaGrange Park, Ill., 1993.

White, R. E., The influence of macropores on the transport of dissolved and suspended matter through soil, *Adv. Soil Sci.*, *3*, 95–120, 1985.

Zhao, L., and R. L. Cerro, Experimental characterization of viscous film flows over complex surfaces, *Int. J. Multiphase Flow*, *18*, 495–516, 1992.

S. R. Sutton, Department of Geophysical Sciences, University of Chicago, Chicago, IL 60637.

T. K. Tokunaga and J. Wan, Earth Sciences Division, Lawrence Berkeley National Laboratory, 1 Cyclotron Road, MS 90-116, Berkeley, CA 94720. (tktokunaga@lbl.gov)

(Received August 3, 1999; revised March 21, 2000;
accepted March 22, 2000.)